MODELING OF INTERCONNECTED FLAT OPEN-CHANNEL FLOW: APPLICATION TO INLAND NAVIGATION CANALS

P. Segovia*[1,2], L. Rajaoarisoa[1], F. Nejjari[2], V. Puig[2], E. Duviella[1]

[1]IMT Lille Douai, Univ. Lille, URIA, F-59000 Lille, France
{pablo.segovia, lala.rajaoarisoa, eric.duviella}@imt-lille-douai.fr

[2]Automatic Control Department, Technical University of Catalonia (UPC), Spain
{fatiha.nejjari, vicenc.puig}@upc.edu

KEY WORDS

Linear model, hydraulic model, Saint-Venant equations, inland waterways.

ABSTRACT

Inland navigation networks are composed of several artificial canals, usually characterized by no slope. These canals are large-scale systems that can be accurately described by means of the nonlinear Saint-Venant partial differential equations. However, the lack of an analytical solution for these equations is one of the reasons why simplified models have been developed. In this work, the Integrator-Delay-Zero model is used as the input-output model to link the water depths to the discharges. A modeling extension for a canal with inflows and outflows along the water stream is proposed: an overlapping problem is discussed and a criterion choice is defined in order to obtain the general model. With regard to this criterion, a calibration step is needed, both to overcome the natural limitations of the simplified model and to ensure the correct computation of the general model. The application of this modeling approach to a part of the inland navigation network in the north of France serves as the case study for this work.

1. INTRODUCTION

Inland navigation networks cover more than 37000 kilometers in Europe and are mainly used for transportation, offering an alternative to the traditional road and rail transport modes (Mallidis, et al., 2012), (Mihic, et al., 2011). An intensification in the use of inland waterways is expected in the near future in France, which will increase the severity of the constraints on the management of the navigation networks.

Inland navigation networks are large-scale systems that are composed of several natural rivers and artificial canals separated by hydraulic structures such as gates or locks that enable the navigation. Reaches are defined as portions of the water stream comprised between two of these structures. In addition, reaches characterized by no slope (otherwise known as flat canals), which are the subject of study in this work, are affected by resonance phenomena caused by the operation of these hydraulic elements. Because of that, waves with a magnitude of several centimeters travel back and forth along the reaches.

The dynamics of a navigation reach can be accurately described by the Saint-Venant's nonlinear partial differential equations (Chow, 1959). However, the lack of an analytical solution for these equations has fostered the development and use of simplified models instead. The Integrator Delay (ID) model was proposed in (Schuurmans, et al., 1999), and it was later improved by considering an additional zero in the transfer function, obtaining the Integrator Delay Zero (IDZ) model, which was compared with the ID model on several canals in (Litrico & Fromion, 2004). More recently, an Integrator Resonance (IR) model was proposed in (van Overloop, et al., 2010) to reproduce the resonance phenomena that affects the dynamics of free-surface water systems. In addition, gray-box models can be used when one or some physical parameters of the system are not well known as in (Horváth, et al., 2014) and (Duviella, et al., 2013). Finally, approaches based on linear parameter-varying models or multi-models that are capable to take into account

* Corresponding author

the nonlinearities that result from considering large operating ranges were presented in (Duviella, et al., 2007), (Duviella, et al., 2010), (Bolea & Puig, 2016) and (Bolea, et al., 2014).

Many inflows and outflows exist along the navigation reaches, and therefore they cannot be considered as simple reaches, which means that the previous simplified models have to be adapted to the particular situation. To overcome these issues, a methodology is proposed in this paper. These reaches are decomposed in several parts, each of them are modeled using IDZ model. Then, an approach is developed to build a global model for the considered reach by interconnecting these different parts.

The paper is structured in the following way: Section 2 presents the modeling of flat open-channels by considering each reach comprised between two water flows (hereinafter referred to as *simple reach*), and then by considering reaches that are characterized by many inflows and outflows (hereinafter referred to as *interconnected reach*). The formulation of a general model that interconnects the simple models is proposed. Some considerations that need to be taken into account when building the global model are discussed and a criterion choice for some terms of the global transfer function matrix is proposed. Section 3 illustrates the modeling methodology by considering part of the inland navigation network in the north of France as the case study for this work. Finally, conclusions about the performed work are drawn in Section 4.

2. FLAT OPEN-CHANNEL MODELING

2.1 Simple reach modeling

As it has been mentioned before, the real dynamics of a canal can be accurately described by the Saint-Venant partial differential equations. However, no analytical solution is known for these equations, which motivates the use of simplified models. Among all the existing options in the literature, the Integrator Delay Zero model proposed in (Litrico & Fromion, 2004) is used in this work. It is obtained as a result of the linearization of the Saint-Venant equations around an operating point called the normal navigation level (NNL) under the assumption of certain conditions, and constitutes a simple yet efficient election to describe the canal dynamics in all regimes.

The structure of the IDZ model is as follows:

$$p_{ij}(s) = \frac{\alpha_{ij}s + 1}{A_{ij}s} e^{-\tau_{ij}s} \tag{1}$$

where α_{ij} represents the inverse of the transfer function zero, A_{ij} is the integrator gain and τ_{ij} is the propagation time delay. It is not possible to compute the exact values of these three parameters; however, a close approximation is given in (Litrico & Fromion, 2004). Hence, the notation $\hat{p}(s)$ replaces $p(s)$ hereinafter.

In low frequencies, the behavior of the canal is similar to a tank that is being filled, and the integrator gain accounts for the change of the water volume according to the variation of the water level. Its value can be approximated by the surface of the canal. The time delay represents the minimum time that a wave needs to travel from its origin to the measurement point. It is well known that canals are affected, to a greater or lesser extent, by resonance phenomena, which causes the waves to travel back and forth, gradually attenuating. Two different time delays have to be computed: τ_d (from upstream to downstream) and τ_u (from downstream to upstream):

$$\tau_d = \frac{L}{C_w + V_w} \tag{2.1}$$

$$\tau_u = \frac{L}{C_w - V_w} \tag{2.2}$$

with L $[m]$ the total length of the canal, C_w the wave celerity $[m/s]$ and V_w the average water velocity $[m/s]$.

The high frequency dynamics are dominated by the zero of (1). However, only the first observed peak in the water level can be predicted, but the resonance phenomena accounts for subsequent, attenuated peaks that the IDZ model is not able to predict.

In general, these parameters are computed for the upstream uniform and the downstream backwater flow parts of the canal, which are then merged into the so-called equivalent parameters that describe the whole

canal. Nevertheless, this work deals with flat canals, which means that there is no upstream uniform flow part, and therefore the parameters only have to be calculated for the backwater part.

The IDZ transfer function is finally used to model any bounded water stream at the upstream and the downstream ends. The MIMO model that represents the influence of the water discharges on the water levels for a reach *r* is given by:

$$\begin{bmatrix} y(0,s) \\ y(L,s) \end{bmatrix} = \boldsymbol{P_r}(s)\boldsymbol{q_r}(s) = \begin{bmatrix} \hat{p}_{11}(s) & \hat{p}_{12}(s) \\ \hat{p}_{21}(s) & \hat{p}_{22}(s) \end{bmatrix} \begin{bmatrix} q(0,s) \\ q(L,s) \end{bmatrix} \tag{3}$$

where 0 and L are the abscissas for the upstream and downstream ends of the reach *r*; $y(0,s)$ and $y(L,s)$, the upstream and downstream water levels; $\hat{p}_{ij}(s)$, the estimation of the IDZ expressions given in (1); and $q(0,s)$ and $q(L,s)$, the upstream and downstream water discharges, respectively.

2.2 Interconnected reach modelling

The previously introduced model for a reach with two inputs (water discharges) and two outputs (water depths) is extended in this section. The aim is to determine the structure of a general system, as well as establishing certain rules that need to be taken into account when building the model.

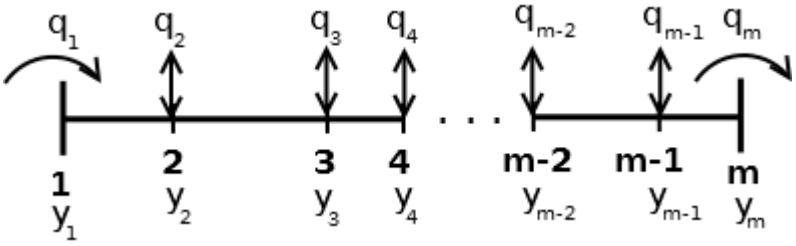

Figure 1: scheme of a reach with *m* sections

Figure 1 depicts a reach with a finite number of intermediate flows (either inflows or outflows) between the initial and final ends of the reach; each of the abscissas in which these flows take place will be called a *section*. It is assumed that all these intermediate flows can be controlled, and thus they are regarded as *m* known inputs of the system. However, it is also considered that it is not always possible to measure the water level for each section, but only for *n* of them ($n \leq m$). This fact justifies the notation introduced in Figure 2.

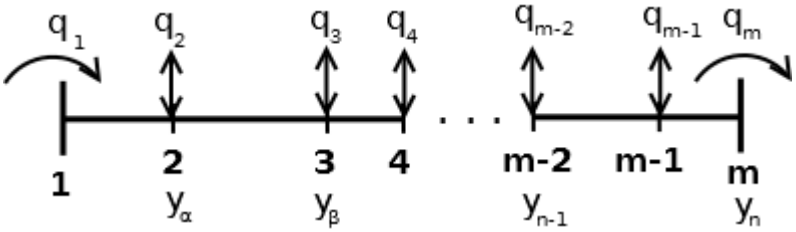

Figure 2: scheme of a reach with only *n* measured water levels

According to Figure 2, the general input-output model is rewritten as follows:

$$\begin{bmatrix} y_\alpha \\ y_\beta \\ \vdots \\ y_n \end{bmatrix} = \boldsymbol{P}(s)\boldsymbol{q}(s) = \begin{bmatrix} \hat{p}_{\alpha 1} & \hat{p}_{\alpha 2} & \cdots & \hat{p}_{\alpha m} \\ \hat{p}_{\beta 1} & \hat{p}_{\beta 2} & \cdots & \hat{p}_{\beta m} \\ \vdots & \vdots & \ddots & \vdots \\ \hat{p}_{n1} & \hat{p}_{n2} & \cdots & \hat{p}_{nm} \end{bmatrix} \begin{bmatrix} q_1 \\ q_2 \\ \vdots \\ q_m \end{bmatrix} \tag{4}$$

where each of the $\hat{p}_{ij}$ elements ($i=\alpha,...,n$; $j=1,...,m$) follows the IDZ structure presented in (1).

To obtain all the $\hat{p}_{ij}$ expressions it is necessary to compute the model (3) between each pair of sections. After that, each of these elements is placed inside matrix $\boldsymbol{P}(s)$ in the position that links the corresponding input/output (I/O) pair. However, the terms that link the input and the output in the same section can be computed more than once, which leads to an *overlapping* problem. In order to clarify this issue, one can consider, for instance, the first section of the reach: the $\hat{p}_{ij}$ expression that links the water depth and the water discharge for the first section can be computed considering the first and the second sections (it will be

$\hat{p}_{11}^{1}$, where the superscript denotes the reach numbering), the first and the third sections ($\hat{p}_{11}^{2}$), the first and the fourth sections ($\hat{p}_{11}^{3}$), and so on.

The position of these overlapped terms inside the matrix $\boldsymbol{P}(s)$ depends on the water levels that can be measured, and therefore no fixed pattern can be established. For the sake of convenience, a new formulation that distinguishes between two types of sections is presented: a first subset of sections for which the water level can be measured and a second one for those whose water level is not measurable. This consideration leads to the alternative formulation shown below:

$$\begin{bmatrix} y_\alpha \\ y_\beta \\ \vdots \\ y_n \end{bmatrix} = \boldsymbol{P}_1(s)\boldsymbol{q}_1(s) + \boldsymbol{P}_2(s)\boldsymbol{q}_2(s) = \begin{bmatrix} \hat{p}_{\alpha\alpha} & \hat{p}_{\alpha\beta} & \cdots & \hat{p}_{\alpha\theta} \\ \hat{p}_{\beta\alpha} & \hat{p}_{\beta\beta} & \cdots & \hat{p}_{\beta\theta} \\ \vdots & \vdots & \ddots & \vdots \\ \hat{p}_{n\alpha} & \hat{p}_{n\beta} & \cdots & \hat{p}_{nn} \end{bmatrix} \begin{bmatrix} q_\alpha \\ q_\beta \\ \vdots \\ q_n \end{bmatrix} + \begin{bmatrix} \hat{p}_{\alpha\mu} & \hat{p}_{\alpha\pi} & \cdots & \hat{p}_{\alpha\omega} \\ \hat{p}_{\beta\mu} & \hat{p}_{\beta\pi} & \cdots & \hat{p}_{\beta\omega} \\ \vdots & \vdots & \ddots & \vdots \\ \hat{p}_{n\mu} & \hat{p}_{n\pi} & \cdots & \hat{p}_{n\omega} \end{bmatrix} \begin{bmatrix} q_\mu \\ q_\pi \\ \vdots \\ q_\omega \end{bmatrix} \quad (5)$$

where the change of notation is due to the fact that a rearrangement of the variables might be necessary.

The representation of this new formulation is depicted in Figure 3:

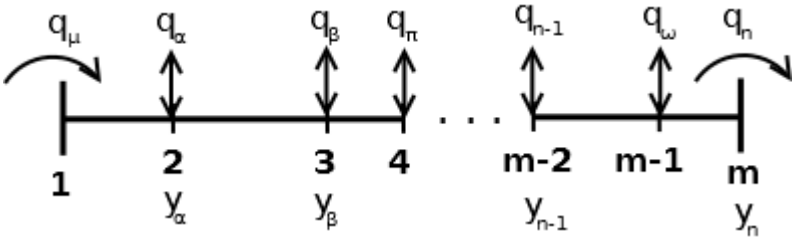

Figure 3: scheme of a reach with notation matching (5)

The interesting fact about this new formulation is that matrix $\boldsymbol{P}(s)$ is split into two matrices $\boldsymbol{P}_1(s)$ and $\boldsymbol{P}_2(s)$, where $\boldsymbol{P}_1(s)$ is a square matrix whose diagonal elements link the I/O pair for the same section; thus, the sought pattern is obtained as the overlapped terms are always placed in this diagonal. The following subsection proposes a choice criterion for these diagonal elements, as well as dealing with other considerations that need to be taken into account when building the general model.

2.2.1 Choice criterion in the overlapping situations

As it has been stated in Section 2.1, there are several possibilities to compute each of the $\hat{p}_{ii}$ terms of $\boldsymbol{P}_1(s)$. It is therefore necessary to determine which one of them will be used and why.

The elements in the diagonal satisfy the property that the time delay is equal to zero; hence, they only consist of a zero and an integrator. The latter is easier to decide on: recall that the physical meaning of the integrator gain is to reproduce the storage of water in low frequencies, similarly as the bottom surface of a tank does when it is being filled. Hence, the total area of the canal should be considered and not any other area comprised between two intermediate sections, which will result in the correct final water level value. This means that a calibration parameter for the integrator gain will be necessary in order to replace the intermediate areas with the total area.

On the other hand, the zero represents the high frequency behavior of the canal. In particular, the IDZ model is only able to predict a first peak, whereas the measured water depth shows subsequent attenuated peaks that account for the resonance phenomenon. According to the notation introduced in (3), it is worth noting that the overlapped terms are always either $\hat{p}_{11}$ or $\hat{p}_{22}$ for a reach comprised between any possible pair of sections. These expressions are given in (Litrico & Fromion, 2004) and depend on the length of the considered reach, which means that a calibration coefficient for the zero is also necessary in order to take into account the entire length of the canal. Moreover, the peak value is very sensitive, which means that even if it is computed for the whole reach, this value still has to be calibrated to match the reference peak value. This procedure is very common when simplified models are used.

With all that in mind, the best strategy to decide among the many available options for an overlapping is to pick the one that considers the two most distant sections as the length will be closer to the total length of the reach and hence the calibration parameters will be closer to the unity. Therefore, the final transfer function that links the water discharge and the water depth for a given section is given by:

$$\hat{p}_{ii}(s) = \frac{k_1 \alpha s + 1}{k_2 A s} \quad (6)$$

with k_1, k_2 being the calibration coefficients. In particular, k_1 will be obtained by means of an optimization procedure in order to fit the first peak of the reference response, while k_2 is just a ratio of the total area of the reach to the area between the considered intermediate sections.

2.2.2 Global sign criterion

The reach is taken as the reference system, which means that inflows are positive as they cause the water level to rise whereas outflows are negative because they have the opposite effect. However, when the different IDZ terms are computed by considering two different sections at a time, a *local* criterion is followed and considers the first flow to be positive and the second one to be negative. This can be easily corrected afterwards by taking care of the signs of the different expressions in the global model: those which link water depths and inflows should be positive while those which link water depths and outflows should be negative.

3. REAL CASE STUDY

This section aims at applying the previous modeling approach to a real system and compare the performance of this model with a reference. In this work, the results provided by SIC^2 (Malaterre, et al., 2014), an hydraulic simulation software that implements the Saint-Venant equations without simplifications, are used as the reference.

After describing the real system, the global model (5) is obtained. Then, scenarios that involve one single lock operation are presented to show the enhancement obtained by means of the calibration step. Finally, a scenario involving a realistic system request is presented to depict the effect of the different overlapped lock operations.

3.1 Description of the System

In this section, the previous general model is obtained for the Cuinchy-Fontinettes reach (CFr), a part of the navigation network in the north of France. This system is supplied at the upstream end by the lock of Cuinchy and emptied at the downstream end by the lock of Fontinettes. At Aire, located halfway between both ends, a lateral gate (not placed inside the CFr) enables the exchange of water between the CFr and a second reach that is not modeled in this work.

The magnitude of each lock operation is given in Table 1. A positive sign for the dispatched water volume means that water flows into the system, while a negative sign implies that the water volume leaves the system. As it can be seen, the largest water volume is dispatched in Fontinettes, and therefore the most important disturbances that are created in this reach are due to the operation of this lock.

Lock operation	**Dispatched water volume** $[m^3]$	**Duration** $[min]$
Cuinchy	3000	15
Aire	4500	15
Fontinettes	-25000	15

Table 1: characteristics of the lock operations

The seaworthiness of the CFr is guaranteed provided that the water level is maintained in the interval 3.8 (NNL) ± 0.15 *m*. Table 2 summarizes the physical and geometrical parameters that characterize the CFr: n_r $[m^{1/3}/s]$ is Manning's roughness coefficient, m (dimensionless) is the side slope of the cross section ($m = 0$ for rectangular shape), q $[m^3/s]$ is the average flow considering a horizon of one day, B_w $[m]$ is the total length of the canal and y_x $[m]$ is the downstream water depth of the reach. Besides, as the canals can be considered flat, the bottom slope s_b is equal to 0.

Reach	n_r	m	B_w	q	L	y_x
Cuinchy - Aire	0.035	0	52	0.6	28700	3.8
Aire - Fontinettes	0.035	0	52	0.6	13600	3.8
Cuinchy - Fontinettes	0.035	0	52	0.6	42300	3.8

Table 2: physical data of the CFr

3.2 Obtaining the CFr model

The next step after presenting the system is to obtain the model that links the water discharges and the water depths in Cuinchy, Aire and Fontinettes. The general expression of this model is as follows:

$$\begin{bmatrix} y_C \\ y_A \\ y_F \end{bmatrix} = \begin{bmatrix} \hat{p}_{11}^G & \hat{p}_{12}^G & \hat{p}_{13}^G \\ \hat{p}_{21}^G & \hat{p}_{22}^G & \hat{p}_{23}^G \\ \hat{p}_{31}^G & \hat{p}_{32}^G & \hat{p}_{33}^G \end{bmatrix} \begin{bmatrix} q_C \\ q_A \\ q_F \end{bmatrix} \tag{7}$$

where y_C, y_A, y_F, q_C, q_A and q_F are the water levels and the water discharges in Cuinchy, Aire and Fontinettes, respectively. In this work, the water level can be measured for all the sections (n = m), and hence the alternative formulation introduced in (5) is not necessary: the overlapped terms are already in the diagonal.

The goal is to determine the global $\hat{p}_{ij}^G$ expressions from the simple models, i.e. considering two sections at a time. These simple models are given by:

$$\begin{bmatrix} y_C \\ y_A \end{bmatrix} = \begin{bmatrix} \hat{p}_{11}^1 & \hat{p}_{12}^1 \\ \hat{p}_{21}^1 & \hat{p}_{22}^1 \end{bmatrix} \begin{bmatrix} q_C \\ q_A \end{bmatrix} \tag{8.1}$$

$$\begin{bmatrix} y_A \\ y_F \end{bmatrix} = \begin{bmatrix} \hat{p}_{11}^2 & \hat{p}_{12}^2 \\ \hat{p}_{21}^2 & \hat{p}_{22}^2 \end{bmatrix} \begin{bmatrix} q_A \\ q_F \end{bmatrix} \tag{8.2}$$

$$\begin{bmatrix} y_C \\ y_F \end{bmatrix} = \begin{bmatrix} \hat{p}_{11}^3 & \hat{p}_{12}^3 \\ \hat{p}_{21}^3 & \hat{p}_{22}^3 \end{bmatrix} \begin{bmatrix} q_C \\ q_F \end{bmatrix} \tag{8.3}$$

The superscripts denote the reach numbering: 1 is used to represent the part comprised between Cuinchy and Aire; 2, between Aire and Fontinettes; and 3, between Cuinchy and Fontinettes, that is, the whole canal. According to this notation, and considering the I/O pair that is linked in each situation, the global model (7) can be rewritten in the following manner:

$$\begin{bmatrix} y_C \\ y_A \\ y_F \end{bmatrix} = \begin{bmatrix} \hat{p}_{11}^1 or\ \hat{p}_{11}^3 & \hat{p}_{12}^1 & \hat{p}_{12}^3 \\ \hat{p}_{21}^1 & \hat{p}_{22}^1\ or\ \hat{p}_{11}^2 & \hat{p}_{12}^2 \\ \hat{p}_{21}^3 & \hat{p}_{21}^2 & \hat{p}_{22}^2\ or\ \hat{p}_{22}^3 \end{bmatrix} \begin{bmatrix} q_C \\ q_A \\ q_F \end{bmatrix} \tag{9}$$

According to the criterion presented in Section 2.2.1, the chosen $\hat{p}_{ij}^G$ term should be the one computed for the longest part in each case. According to the lengths given in Table 2, (9) can be finally rewritten as:

$$\begin{bmatrix} y_C \\ y_A \\ y_F \end{bmatrix} = \begin{bmatrix} \hat{p}_{11}^3 & \hat{p}_{12}^1 & \hat{p}_{12}^3 \\ \hat{p}_{21}^1 & \hat{p}_{22}^1 & \hat{p}_{12}^2 \\ \hat{p}_{21}^3 & \hat{p}_{21}^2 & \hat{p}_{22}^3 \end{bmatrix} \begin{bmatrix} q_C \\ q_A \\ q_F \end{bmatrix} \tag{10}$$

In addition, the distinction between inflows and outflows has to be pointed out: q_C and q_A are inflows whereas q_F is an outflow. The easiest way to simulate this situation consists in considering all of them as inflows but then adding a negative sign to the terms that are multiplied by the outflows. Thus, the expressions in the 1st and 2nd columns must be positive, while those in the 3rd column must be negative.
Besides, the calibration strategy presented in (6) has to be taken into account when building (10). It is worth mentioning that no calibration coefficient for the integrator gain is needed for the $\hat{p}_{ij}^3$ terms; indeed, the integrator gain for these terms has been computed with the value of the total length C-F.

Finally, the resulting numerical model (10) after taking into account all the previous considerations is given by:

$$\begin{bmatrix} y_C \\ y_A \\ y_F \end{bmatrix} = \begin{bmatrix} \frac{6341s+1}{2.2e6\,s} & \frac{5909s+1}{2.2e6\,s}e^{-4703s} & -\frac{5819\,s+\,1}{2.2e6\,s}e^{-6931s} \\ \frac{5423s+1}{2.2e6\,s}e^{-4698s} & \frac{2546s+1}{2.2e6\,s} & -\frac{4201s+1}{2.2e6\,s}e^{-2229s} \\ \frac{10450s+1}{2.2e6\,s}e^{-6924s} & \frac{5218s+1}{2.2e6\,s}e^{-2226s} & -\frac{7209s+1}{2.2e6\,s} \end{bmatrix} \begin{bmatrix} q_C \\ q_A \\ q_F \end{bmatrix} \quad (11)$$

3.3 Simulation of Single Input Scenarios

In this section, different scenarios with one input at a time are presented. The objective is to show the enhancement obtained by applying the calibration step described in (6) that results in the model given by (11). The three considered experiments depict the reference water level and the predicted water levels with and without model calibration. Moreover, to ensure a quantitative comparison, the Nash-Sutcliffe model efficiency coefficient (Nash & Sutcliffe, 1970) is used to assess the predictive power of the two models as follows:

$$E = 1 - \frac{\sum_{t=1}^{T}[Y_0(t) - Y_m(t)]^2}{\sum_{t=1}^{T}[Y_0(t) - \bar{Y}_o]^2} \quad (12)$$

with T the time period for which the data have been acquired, $Y_0(t)$ the observed water depth at time t, $Y_m(t)$ the predicted water depth at time t and $\bar{Y}_o$ the mean value of the observed water depths, respectively. E can range from 1 to -∞, where 1 indicates a perfect match of modeled and observed values, 0 corresponds to the case in which the model predictions are as accurate as the mean of observed data and $E < 0$ means that the model predictions are less accurate than the mean of observed data.

Figures 4, 5 and 6 are adjusted to display properly the peak response, even if the simulation lasts longer. As the final water level has also been calibrated but cannot be displayed properly in the same figure, its value is also given at the end of each simulation (which can be considered to be the stationary value).

A final remark before proceeding with all the scenarios is that the expressions given in (10) can be classified into two groups: some expressions (namely $\hat{p}_{11}^G$, $\hat{p}_{13}^G$, $\hat{p}_{31}^G$ and $\hat{p}_{33}^G$) are taken from the third simple model, which uses the entire length of the canal, whereas the others are taken from either the first or the second simple models. This means that the calibration step should be less necessary for the terms in the first group than for the terms in the second group.

3.3.1 Input in Cuinchy

A lock operation in Cuinchy is simulated at time t = 1h. The water levels in Cuinchy, Aire and Fontinettes are presented in Figure 4:

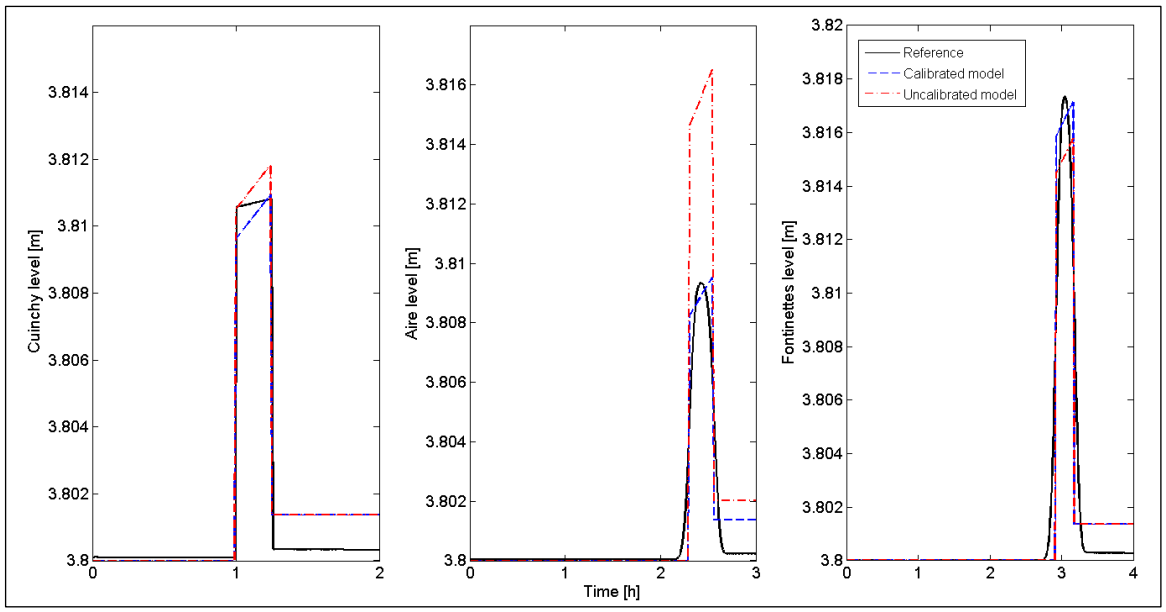

Figure 4: peak responses for a lock operation in Cuinchy

Figure 4 shows how the calibration step is almost not necessary for the correct prediction of the water levels in Cuinchy and Fontinettes, but it is not the case for the water level in Aire, as it is originally quite far from the reference.

		y_C	y_A	y_F
Nash-Sutcliffe coefficient	Calibration	0,699	0,7807	0,8182
	No calibration	0,6665	-1,8901	0,7955
Final water level $[m]$	Reference	3,8014		
	Calibration	3,8014		
	No calibration	3,8014	3,8020	3,8014

Table 3: Nash-Sutcliffe coefficients and final water levels

In this situation, both $\hat{p}_{11}^{G}$ and $\hat{p}_{13}^{G}$ come from (8.3), which means that the corresponding prediction of the water levels should be close to the reference. Indeed, both the Nash-Sutcliffe coefficients and the final water level given in Table 3 show how the two models yield almost the same results, whereas the improvement obtained by the calibration step in predicting the water level in Aire is much more notorious.

On the other hand, it is worth noting that the final water levels for the uncalibrated model must not necessarily all agree on the same value, as they have been computed for different simple reaches and each of them considers a different length. Therefore, by calibrating the integrator gain, the same final water level for all the sections is obtained, which makes sense as the canal is flat.

3.3.2 Input in Aire

A lock operation in Aire is simulated at time t = 1h. The water levels in Cuinchy, Aire and Fontinettes are presented in Figure 5:

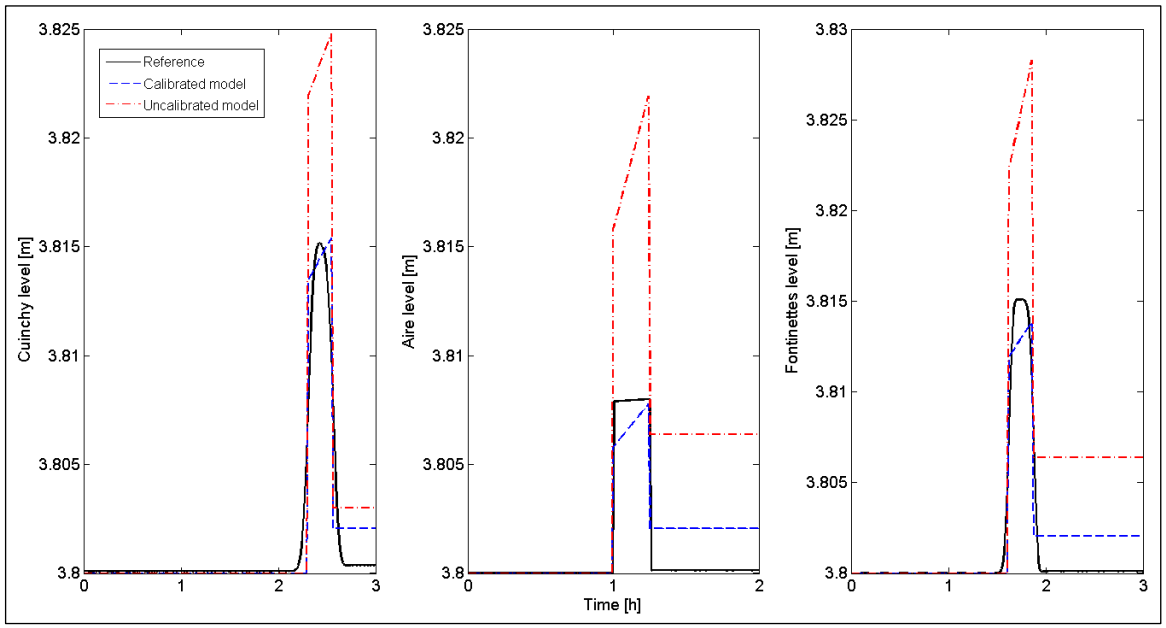

Figure 5: peak responses for a lock operation in Aire

In this case, none of the used expressions $\hat{p}_{21}^{G}$, $\hat{p}_{22}^{G}$ and $\hat{p}_{23}^{G}$ comes from the third simple model and the calibration step is clearly needed in the prediction of the three water levels, according to the results given in Figure 5.

		y_C	y_A	y_F
Nash-Sutcliffe coefficient	Calibrated model	0,6738	0,6566	0,8559
	Uncalibrated model	-2,1514	-10,1550	-1,4038
Final water level [*m*]	Reference	3,8021		
	Calibrated model	3,8021		
	Uncalibrated model	3,8030	3,8064	3,8064

Table 4: Nash-Sutcliffe coefficients and final water levels

Table 4 gathers all the computed coefficients for this scenario. It is shown how the calibration procedure clearly improves the predictive power of the model: indeed, the three Nash-Sutcliffe coefficients were negative before the calibration step, which means that even the means of the reference water levels were a better predictor than the computed model.

3.3.3 Input in Fontinettes

A lock operation in Fontinettes is simulated at time t = 1h. The water levels in Cuinchy, Aire and Fontinettes are presented in Figure 6:

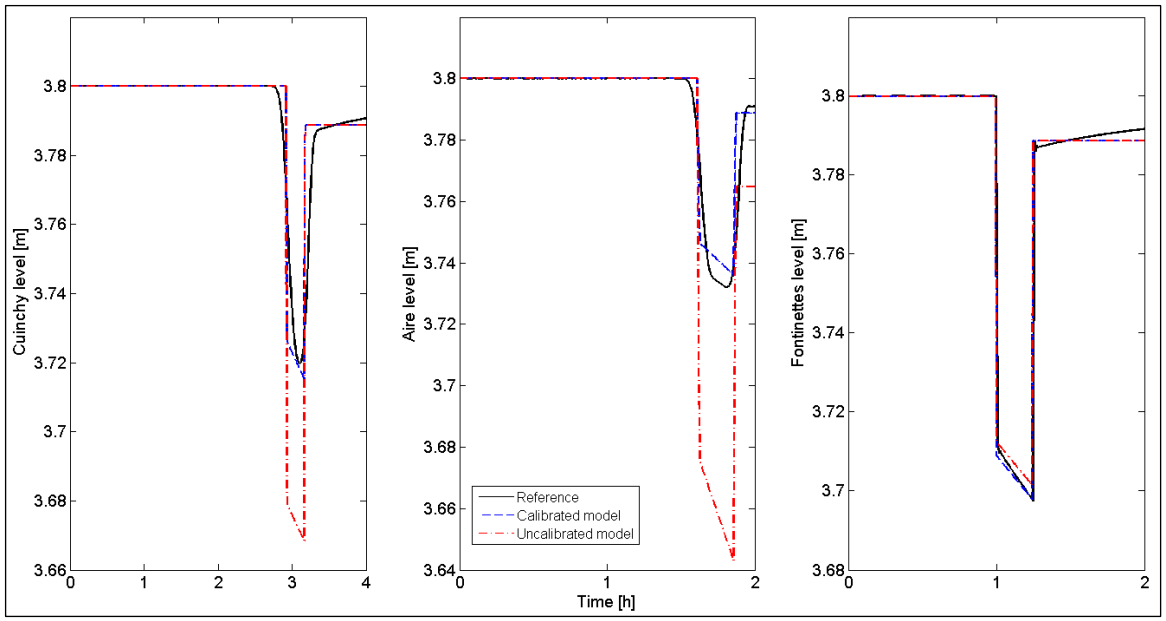

Figure 6: peak responses for a lock operation in Fontinettes

According to what was said in the final remark before presenting the different scenarios, the calibration step was not expected to be necessary for the water level in Cuinchy and yet it is, according to the results presented in Figure 6. This fact justifies the statement in Section 2.2.1 about the need for calibration when simplified models were used.

		y_C	y_A	y_F
Nash-Sutcliffe coefficient	Calibrated model	0,4788	0,7555	0,7048
	Uncalibrated model	-1,2591	-4,9139	0,6704
Final water level [*m*]	Reference	3,7886		
	Calibrated model	3,7886		
	Uncalibrated model	3,7886	3,7646	3,7886

Table 5: Nash-Sutcliffe coefficients and final water levels

The computed coefficients for this scenario are summarized in Table 5. Both the water depths in Cuinchy and Aire are much better predicted after the calibration step. The difference is that, while the former has to be done to compensate the limitations of the simplified model, the latter was expected from the beginning due to the use of a partial length instead of the total one.

3.4 Simulation of a Realistic Scenario

After verifying that the calibration strategy improves, indeed, the predictive power of the models, the realistic scenario depicted below is considered. Each lock operation corresponds to one boat crossing the gate; the lock is used to raise or lower the boat that is using that gate. According to the real operating schedule, boats are allowed to navigate through gates from 6 am to 8 pm, which accounts for the considered 14-hour horizon. In this scenario, 13 boats enter the CFr through the gate of Cuinchy: 10 of them leave the system through the gate of Fontinettes while the remaining boats use the gate of Aire to exit the CFr.

Figure 7 represents the set of lock operations in each section, and they are defined as the ratio of the dispatched water volumes to the duration of these operations. These two magnitudes were given in Table 1.

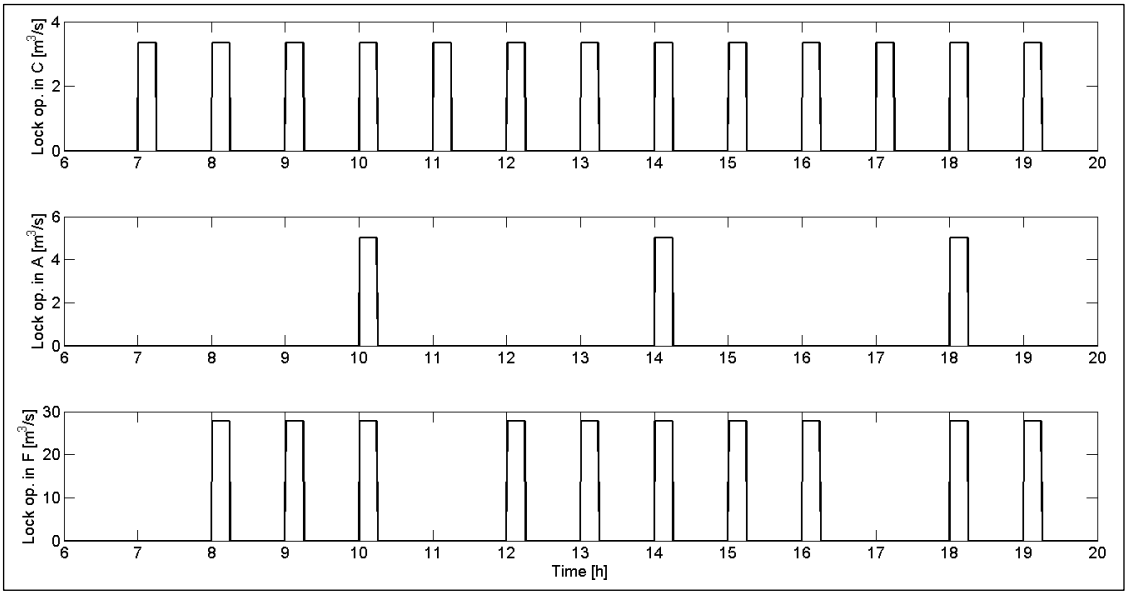

Figure 7: realistic schedule of lock operations

According to the inputs considered for this scenarios, the water levels in the three sections are depicted in Figure 8.

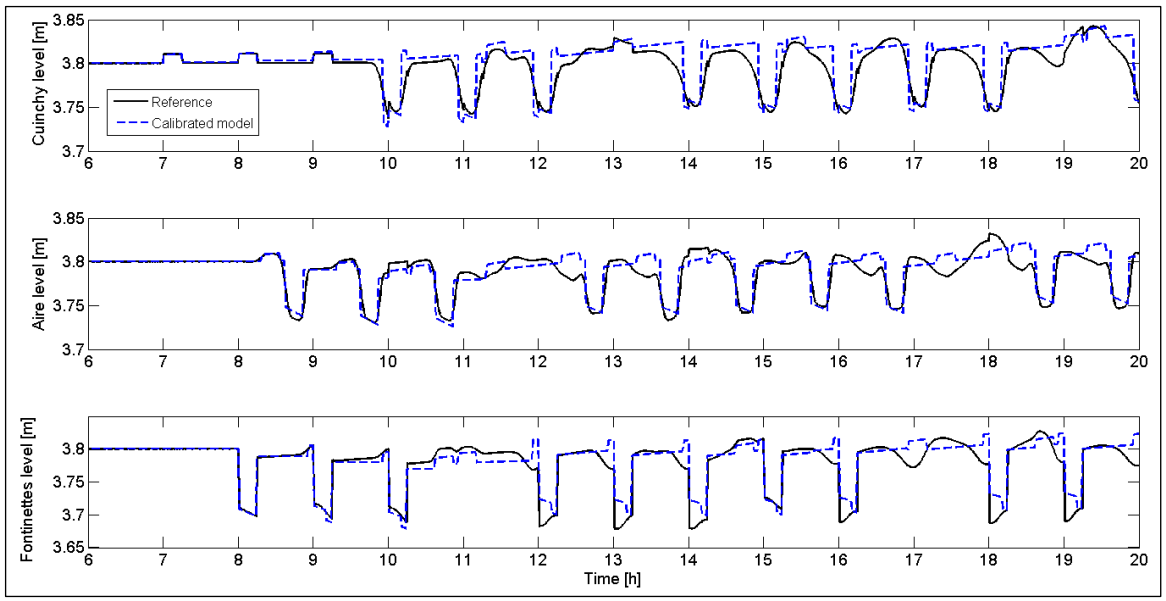

Figure 8: measured and predicted water levels

The simulation of this realistic scenario aims at illustrating the interacting effect of different waves that collide along the water stream. According to Table 1, the magnitude of the operations in the lock of Fontinettes is much bigger than the other two and hence the effect of these actions dominates the global behavior of the system. For instance, the first lock operation in Fontinettes takes place at 8 am: according to the time τ_{13}^{G} delay given in (10), around two hours are needed to perceive the effect of this action in Cuinchy. Indeed, it can be seen how the water level in that place starts decreasing around 10 am. Moreover, there is a lock operation in Cuinchy at the same time, but its effect is blurred since its magnitude is much smaller than the magnitude of the lock operation in Fontinettes.

On the other hand, it can be seen how the final model (10) is able to accurately predict the water level given by the reference. There are certain moments in which one or some of the water levels do not exactly match the reference, but this behavior is explained by the fact that the used IDZ model is a simplification of the real dynamics of the canal, and therefore it will never be able to capture all the details.

4. CONCLUSIONS AND FUTURE WORK

This work presented the modeling of interconnected flat navigation canals. First, the linearized IDZ model was presented for a reach with two inputs and two outputs at the ends of the reach. Then, this model was extended for the general case in which intermediate inflows and/or outflows might be found along the water stream: the overlapping problem was discussed and a criterion choice was proposed. In addition, a calibration procedure was introduced after the criterion choice to ensure that the entire length of the canal was taken into account for all the terms in the global model. This step is necessary since these expressions are computed by considering each pair of sections (the discharges and water levels for these sections), and thus the entire length of the canal is not considered except in one case. Finally, the proposed modeling approach was exemplified in two steps by using the Cuinchy-Fontinettes navigation reach: in the first one, three scenarios with just one lock operation at a time are considered to illustrate the importance of the calibration step. After that, a realistic scenario was designed to test the accuracy of the model when the effects of lock operations in different sections are mixed up.

Further work is expected to be carried out from these models; in particular, in fault detection and isolation (FDI) and fault-tolerant control (FTC). In addition, other models that take into account the resonance phenomena in their formulation such as the Integrator Resonance (IR) model will be investigated.

REFERENCES AND CITATIONS

Bolea, Y. & Puig, V., 2016. Gain-scheduling multivariable LPV control of an irrigation canal system. *ISA Transactions*, Volume 63, pp. 274-280.

Bolea, Y., Puig, V. & Blesa, J., 2014. Linear parameter varying modeling and identification for real-time control of open-flow irrigation canals. *Environmental modelling & software,* Volume 53, pp. 87-97.

Chow, V., 1959. *Open-channels hydraulics.* New York: McGraw-Hill.

Duviella, E., Bako, L. & Charbonnaud, P., 2007. Gaussian and boolean weighted models to represent variable dynamics of open channel systems. *46th IEEE Conference on Decision and Control,* pp. 3084-3089.

Duviella, E. et al., 2013. Inland navigation channel model: application to the Cuinchy-Fontinettes reach.. *Networking, Sensing and Control (ICNSC),* pp. 164-169.

Duviella, E. et al., 2010. Supervised gain-scheduling multimodel versus linear parameter-varying internal model control of open-channel systems for large operating conditions. *Journal of Irrigation and,* 136(8), pp. 543-552.

Horváth, K. et al., 2014. Gray-box model of inland navigation channel: application to the Cuinchy-Fontinettes reach. *Journal of Intelligent Systems,* 23(2), pp. 183-199.

Litrico, X. & Fromion, V., 2004. Simplified modeling of irrigation canals for controller design. *Journal of Irrigation and Drainage Engineering,* 130(5), pp. 373-383.

Malaterre, P., Dorchies, D. & Baume, J., 2014. Automatic tuning of robust PI controllers for a cascade of rivers or irrigation canals pools. *IEEE European Control Conference (ECC),* pp. 2780-2785.

Mallidis, I., Dekker, R. & Vlachos, D., 2012. The impact of greening on supply chain design and cost: a case for a developing region. *Journal of Transport Geography,* Volume 22, pp. 118-128.

Mihic, S., Golusin, M. & Mihajlovic, M., 2011. Policy and promotion of sustainable inland waterway transport in Europe - Danube River. *Renewable and Sustainable Energy Reviews,* 15(4), pp. 1801-1809.

Nash, J. & Sutcliffe, J., 1970. River flow forecasting through conceptual models part I - A discussion of principles. *Journal of hydrology,* 10(3), pp. 282-290.

Schuurmans, J. et al., 1999. Modeling of irrigation and drainage canals for controller design. *Journal of Irrigation and Drainage Engineering,* 125(6), pp. 338-344.

van Overloop, P. et al., 2010. Identification of resonance waves in open water channels. *Control Engineering Practice,* 18(8), pp. 863-872.